

## Cellular Binding of Hepatitis C Virus Envelope Glycoprotein E2 Requires Cell Surface Heparan Sulfate\*

Received for publication, March 5, 2003, and in revised form, July 15, 2003  
Published, JBC Papers in Press, July 16, 2003, DOI 10.1074/jbc.M302267200

Heidi Barth‡, Christiane Schäfer‡, Mohammed I. Adah‡§, Fuming Zhang¶, Robert J. Linhardt¶, Hidenao Toyoda||, Akiko Kinoshita-Toyoda||, Toshihiko Toida||, Toin H. van Kuppevelt\*\*, Erik Depla‡‡, Fritz von Weizsäcker‡, Hubert E. Blum‡, and Thomas F. Baumert‡‡§§

From the ‡Department of Medicine II, University of Freiburg, D-79106 Freiburg, Germany, the ¶Departments of Chemistry, Medicinal and Natural Products Chemistry, and Chemical and Biochemical Engineering, University of Iowa, Iowa City, Iowa 52242, the ||Department of Analytical Chemistry, Chiba University, Chiba 263-8522, Japan, the \*\*Department of Biochemistry, NCMLS, University Medical Center, 6500HB Nijmegen, The Netherlands, and ‡‡Innogenetics N. V., B-9052 Ghent, Belgium

**The conservation of positively charged residues in the N terminus of the hepatitis C virus (HCV) envelope glycoprotein E2 suggests an interaction of the viral envelope with cell surface glycosaminoglycans. Using recombinant envelope glycoprotein E2 and virus-like particles as ligands for cellular binding, we demonstrate that cell surface heparan sulfate proteoglycans (HSPG) play an important role in mediating HCV envelope-target cell interaction. Heparin and liver-derived highly sulfated heparan sulfate but not other soluble glycosaminoglycans inhibited cellular binding and entry of virus-like particles in a dose-dependent manner. Degradation of cell surface heparan sulfate by pretreatment with heparinases resulted in a marked reduction of viral envelope protein binding. Surface plasmon resonance analysis demonstrated a high affinity interaction ( $K_D$   $5.2 \times 10^{-9}$  M) of E2 with heparin, a structural homologue of highly sulfated heparan sulfate. Deletion of E2 hypervariable region-1 reduced E2-heparin interaction suggesting that positively charged residues in the N-terminal E2 region play an important role in mediating E2-HSPG binding. In conclusion, our results demonstrate for the first time that cellular binding of HCV envelope requires E2-HSPG interaction. Docking of E2 to cellular HSPG may be the initial step in the interaction between HCV and the cell surface resulting in receptor-mediated entry and initiation of infection.**

Hepatitis C virus (HCV)<sup>1</sup> is a major cause of chronic hepatitis worldwide (1, 2). Most HCV-infected individuals develop

chronic hepatitis that may progress to liver cirrhosis and hepatocellular carcinoma. A vaccine for prevention of infection is not available and treatment options for chronic HCV infection are limited (2, 3). Therefore, novel antiviral treatment strategies are needed.

HCV has been tentatively classified in a separate genus (hepacivirus) of the *Flaviviridae* family (4). The virion contains a positive-sense single-stranded RNA genome of about 9.5 kb. The genome encodes a single polyprotein of 3,010 to 3,030 amino acids that is processed into functional proteins by host and viral proteases (4–6). The structural proteins comprise the core protein forming the viral nucleocapsid and two envelope glycoproteins, E1 and E2 (5, 6). Enveloped virions have been visualized in infected target cells (5, 7). Several lines of evidence have demonstrated that the HCV envelope proteins may play a crucial role in the initiation of infection by mediating virus-host cell membrane interaction. E2 is thought to initiate viral attachment (6, 8, 9), whereas E1 may be involved in virus-cell membrane fusion (6, 9). Several cell surface proteins, the tetraspanin CD81 (10, 11), the LDL receptor (12), the asialoglycoprotein receptor (13) and scavenger receptor B1 (14), have been proposed to play a role in mediating E2 binding and/or HCV internalization. However, it is still unclear whether any of these molecules can act as a functional cellular receptor mediating viral entry and initiation of infection. The study of HCV envelope binding, membrane fusion, and cellular entry has been hampered by the lack of a cell culture system for the large scale synthesis of infectious virions.

The HCV structural proteins have been shown to assemble into hepatitis C virus-like particles (HCV-LPs) with morphological, biophysical, and antigenic properties similar to putative virions from infected humans (15–23). VLPs have been successfully used as a surrogate model to study the host cell membrane interaction of several viruses (24–27). In line with these observations, we and others have demonstrated that the interaction of insect cell-derived HCV-LPs with defined human cells lines and hepatocytes represents a convenient high-throughput model system for studying viral binding and entry (18, 19, 23).

Glycosaminoglycan (GAG) chains on cell surface proteoglycans provide primary docking sites for the binding of various viruses and other microorganisms to eukaryotic cells. GAGs are present almost ubiquitously on cell surfaces but vary with

\* This work was supported in part by grants from the European Union, Brussels, Belgium QLK2-CT-1999-00356 and QLK2-CT-2002-01329, the Wilhelm Sander-Stiftung, Munich, Germany (99041.1), and the Deutsche Forschungsgemeinschaft (Ba1417/9-1). The costs of publication of this article were defrayed in part by the payment of page charges. This article must therefore be hereby marked "advertisement" in accordance with 18 U.S.C. Section 1734 solely to indicate this fact.

§ Supported by a Georg Forster fellowship of the Alexander von Humboldt-Foundation, Bonn, Germany.

§§ To whom correspondence should be addressed: Dept. of Medicine II, University of Freiburg, Hugstetter Strasse 55, D-79106 Freiburg, Germany. Tel.: 49-761-270-3401; Fax: 49-761-270-3259; E-mail: tbaumert@ukl.uni-freiburg.de.

<sup>1</sup> The abbreviations used are: HCV, hepatitis C virus; Ac, acetyl; BSA, bovine serum albumin; CSF, classical swine fever; ΔUA, 4-deoxy-α-L-threo-hex-4-enopyranosyluronic acid; E1/E2, envelope glycoprotein 1 and 2; EDC, N-ethyl-N-(dimethylaminopropyl) carbodiimide; ELISA, enzyme-linked immunosorbent assay; GAGs, glycosaminoglycans; GlcN, 2-amino-2-deoxyglucopyranose; HS, heparan sulfate; HVR, hypervariable region; IgG, immunoglobulin G; KS, keratan sulfate; LDL,

low density lipoprotein; MFI, mean fluorescence intensity; NC, negative control; NHS, N-hydroxysuccinimide; NS5A/NS5B, nonstructural protein 5A and 5B; PBS, phosphate-buffered saline; PE, phycoerythrin; RU, resonance unit; SPR, surface plasmon resonance; TBE, tick-borne encephalitis; UA, pyranosyluronic acid; VLPs, virus-like particles.

respect to their composition and quantity among different species, cell types, tissues, and cellular development stages (28). The GAG heparan sulfate is an important initial cellular binding molecule for several viruses. These viruses include several members of the *Flaviviridae* family such as Dengue (29–31), classical swine fever (CSF) (32), and tick-borne encephalitis (TBE) (33) viruses as well as herpes simplex virus 1 (34), human herpesvirus 8 (35), and papilloma virus (24). It has been proposed that the affinity of the viral surface molecules to heparan sulfate may be an important determinant for tissue tropism and pathogenicity (36, 37). Apart from mediating virus binding to target cells, heparan sulfate carrying a specific sulfation pattern can also act as a cell surface receptor mediating entry of herpes simplex virus type 1 (34, 37).

A comparative structural analysis of the E2 protein of various HCV isolates demonstrated that positively charged amino acid residues are highly conserved in the N terminus of E2 hypervariable region 1 (38). This finding led to the conclusion that E2 may bind to negatively charged compounds such as cell surface GAGs. In this study, we demonstrate for the first time that E2 interacts with highly sulfated heparan sulfate and that this interaction plays a major functional role in mediating cellular binding of HCV glycoprotein E2 to target cells.

#### EXPERIMENTAL PROCEDURES

**Reagents and Cell Lines**—HCV-LPs of genotypes 1a and 1b were synthesized and purified as described (15, 18). HCV-LP E2 concentration was determined as described (18). Recombinant C-terminal-truncated envelope glycoprotein E2 (comprising amino acids 384–673) and E2 containing a deletion of HVR1 ( $\Delta$ E2; comprising amino acids 412–715) were generated using recombinant vaccinia viruses containing HCV envelope cDNAs of a European HCV 1b isolate (39). Recombinant NS5A and NS5B proteins (Mikrogen Corp., Martinsried, Germany) were generously provided by H. Diepolder, Dept. of Medicine II, University of Munich. Heparin, kidney-derived normally sulfated heparan sulfate, keratan sulfate, dextran sulfate, chondroitin sulfate, dermatan sulfate, chondroitin ABC lyase, and heparinases I and III were obtained from Sigma-Aldrich Corp. Highly sulfated liver-derived heparan sulfate was isolated as previously described (40). Mouse anti-E2 (16A6) monoclonal antibody has been described previously (18). Monoclonal antibodies directed against NS5A and NS5B proteins were provided by J. Y. N. Lau (Schering-Plough Corporation, Kenilworth, NJ). Origin and maintenance of HepG2, HuH-7, MOLT-4, and Daudi cells have been described (18).

**Analysis of Envelope Protein-Heparin Interaction by ELISA**—96-well ELISA plates (Immulon 2 HB, Thermo Labsystems, Helsinki, Finland) were coated with 1  $\mu$ g of heparin-bovine serum albumin (BSA) or BSA (Sigma) per well at 4 °C overnight and then incubated with blocking buffer (5% nonfat dry milk in PBS, 0.1% Tween-20) for 1 h at room temperature. HCV-LPs or recombinant HCV proteins were added and incubated for 1 h at 37 °C. After washing, heparin- or BSA-bound proteins were detected by the addition of mouse anti-envelope or anti-NS5A/B monoclonal antibodies (dilution 1:500 in PBS; 45 min at 37 °C). The plates were then incubated with horseradish peroxidase-conjugated goat anti-mouse IgG secondary antibody (dilution 1:1,000 in PBS; 30 min at 37 °C). Protein-bound antibodies were detected by colorimetry as described recently (41). The plates were washed six times with PBS and with 0.1% Tween-20 between each step.

**Measurement of Envelope Protein-Heparin Interaction by SPR**—SPR measurements were performed on a BIAcore 3000 system (BIAcore AB, Uppsala, Sweden) using the BIAcore 3000 version software. Pioneer Sensor C1 Chips (BIAcore AB) with a flat carboxymethylated surface were used in this study to reduce nonspecific binding. BSA-heparin (Sigma) was covalently immobilized to the sensor surface (Fc2) through its primary amino groups (42). In brief, the carboxymethyl groups on the chips surface were first activated using an injection pulse 10 min (50  $\mu$ l, with the flow rate 5  $\mu$ l/min) of an equimolar mix of *N*-hydroxysuccinimide (NHS) and *N*-ethyl-*N*-(dimethylaminopropyl) carbodiimide (EDC) (final concentration is 0.05 M, mixed immediately prior to injection). A solution of BSA-heparin (obtained from Sigma; 200  $\mu$ g/ml in sodium acetate buffer with the addition of 2 M guanidine, pH 4.0), was then applied (20  $\mu$ l) by manual injection. Excess unreacted sites on the sensor surface were blocked by injection with 50  $\mu$ l of 1 M ethanolamine. The successful immobilization of BSA-heparin was confirmed by the

observation of an  $\sim$ 250 RU increase in the sensor chip. To prepare the control flow cell (Fc1), BSA (Amresco, Solon, OH) was immobilized on the surface with a similar amine coupling procedure. After the surface was activated with NHS/EDS, 5  $\mu$ l of BSA solution (20  $\mu$ g/ml in sodium acetate buffer, pH 4.0) were injected manually to obtain 250 RU immobilized.

Measurement of heparin-protein interaction was performed as follows: different dilutions of protein samples in PBS containing 0.05% betaine were injected (30  $\mu$ l) at a flow rate of 10  $\mu$ l/min. At the end of the sample injection, the same buffer flew over the sensor surface to facilitate dissociation. After a 3-min dissociation time, the sensor surface was regenerated by injecting first with 10  $\mu$ l of 2 M NaCl, then with 10  $\mu$ l of glycine-HCl, pH 2 buffer (BIAcore) and 10  $\mu$ l of NaOH 50 (BIAcore). The response was monitored as a function of time (sensorgram) at 25 °C.

**Analysis of Binding of HCV-LP E2 and Recombinant E2 to Human Cell Lines by Flow Cytometry**—To investigate whether binding of HCV-LP E2 or recombinant E2 can be blocked by soluble GAGs, HCV-LPs (corresponding to an E2 concentration of 2.5  $\mu$ g/ml) or recombinant E2 (2.5  $\mu$ g/ml) were preincubated with defined GAGs at various concentrations for 20 min at room temperature in Dulbecco's PBS (Invitrogen). Protein-GAG complexes were added to cells ( $1.5 \times 10^5$  cells per assay), and cellular binding of HCV-LP and recombinant E2 was analyzed by flow cytometry using monoclonal antibodies as described (18). For pretreatment with GAG lyases, HepG2 cells were removed from culture plates by incubation in PBS containing 5 mM EDTA as described (29). HepG2 or MOLT-4 cells ( $1.5 \times 10^5$  cells per assay) were then incubated in Dulbecco's PBS or 20 mM Tris-HCl, 50 mM NaCl, 4 mM CaCl<sub>2</sub>, 0.01% BSA, pH 6.8 (24) containing heparinase I, heparinase III, or chondroitin ABC lyase. After incubation for 1 h at 37 °C, the cells were put on ice and washed once with ice-cold PBS. HCV-LPs and E2 were added to pretreated cells, and HCV-LP or E2 binding was analyzed as described above.

**Inhibition of Cellular GAG Sulfation by Sodium Chlorate**—To reduce the extent of sulfation of heparan sulfate on the cell surface, HepG2 cells were cultured for 48 h in the presence of the sulfation inhibitor sodium chlorate as described (24). In parallel experiments, cells were supplemented with sodium sulfate (2 mM) for 48 h to assess the sulfation specificity of inhibition of HCV-LP binding. HCV-LP E2 binding to HepG2 cells after sodium chlorate treatment and addition of sodium sulfate was analyzed by flow cytometry as described above.

**Analysis of HCV-LP Internalization**—HCV-LPs were preincubated with or without heparin (10  $\mu$ g/ml in Dulbecco PBS) as described above. HCV-LP binding was measured by incubation of HepG2 cells (grown on cover slides) with HCV-LP or HCV-LP-heparin complexes at 4 °C for 40 min. For temperature-dependent HCV-LP entry, cells were incubated for additional 60 min at 37 °C. After removal of non-bound HCV-LPs by washing with ice-cold PBS, cells were fixed with PBS containing 3.5% paraformaldehyde and permeabilized using PBS containing 0.1% Triton X-100. Cells were stained for HCV-LP binding and entry using mouse anti-E2 antibody 16A6 (dilution 1:100 in PBS) and Cy3-conjugated anti-mouse IgG (Dianova, Hamburg, Germany; dilution 1:250 in PBS). For the co-staining of the cytoskeleton, cells were co-incubated with a polyclonal rabbit anti-actin antibody (Sigma-Aldrich; dilution 1:200 in PBS) and FITC-conjugated anti-rabbit IgG (ICN Biomedicals, Costa Mesa, CA; dilution 1:500 in PBS). Between antibody incubations (1 h at room temperature) cells were washed three times in PBS. For co-staining of the nucleus, cells were incubated with DRAQ-5 (Biostat; Leicestershire, UK), a highly permeable DNA-interactive agent, according to the manufacturer's protocol. Prior to analysis by confocal laser scanning microscopy, cover slides were mounted in antifade reagent (Fluoroguard, Bio-Rad) to minimize photobleaching. Stained cells were analyzed using a Zeiss LSM 410 laser scanning confocal microscope (Carl Zeiss Corp., Jena, Germany) with argon (488 nm) and helium/neon (543 and 633 nm) lasers. Digitalized images were analyzed using Zeiss-LSM Image Browser version 2.8 (Carl Zeiss Corp.).

**Immunostaining of Cell Surface Heparan Sulfate by Single Chain Antibodies**—To assess whether HepG2 and MOLT-4 cells express highly sulfated heparan sulfate on their cell surface, HepG2 and MOLT-4 cells were incubated with VSV-tagged single chain anti-heparan sulfate antibody HS4C3 (bacterial periplasmic fraction diluted 1:2 in PBS/BSA, incubation time 90 min). HS4C3 has been shown to interact with highly sulfated heparan sulfate on a variety of tissues (43). Parallel incubation of cells with VSV-tagged single chain antibody MPB49 served as a negative control. Control antibody MPB49 was selected for its similar amino acid sequence compared with HS4C3 (Vh3



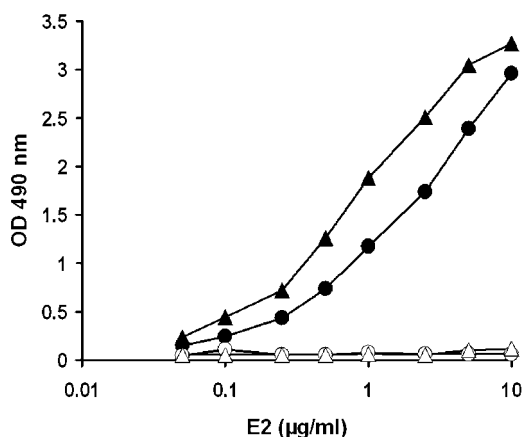


FIG. 1. Interaction of HCV-LP envelope glycoprotein E2 (HCV-LP E2) and recombinant E2 with heparin. ELISA plates were coated with BSA-heparin (closed symbols) or BSA (open symbols) as described under "Experimental Procedures." HCV-LP E2 (▲, △) and recombinant E2 (●, ○) were added in the concentrations indicated on the x-axis (final volume, 100  $\mu$ l). After removal of non-bound E2 by extensive washing with PBS, heparin- or BSA-bound E2 was detected using monoclonal anti-E2 and horseradish peroxidase-conjugated anti-mouse IgG antibodies. Bound antibodies were detected by colorimetric reaction. The optical density (OD) of the colorimetric reaction is proportional to heparin-BSA or BSA-bound E2. Mean values of duplicate measurements of a representative experiment are shown.

family and DP 38 gene number) and does not recognize a defined epitope.<sup>2</sup> For detection of bound antibodies, cells were incubated with Cy3-labeled mouse anti-VSV antibody P5D4 (Sigma-Aldrich; 1:100 in PBS/BSA; 1-h incubation time). Between antibody incubations cells were washed three times in PBS. Labeled cells were then analyzed by flow cytometry or laser scanning confocal microscopy as described above.

**Analysis of Cellular Heparan Sulfate Structure and Sulfation**—Disaccharide analysis of cell surface heparan sulfate from freeze-dried HepG2 and MOLT-4 cells using was performed using high performance liquid chromatography with post-column fluorescence detection as previously described (44, 45). Analysis of kidney and liver heparan sulfate by capillary electrophoresis has been recently described (40).

## RESULTS

**High Affinity Interaction of Envelope Glycoprotein E2 with the Heparan Sulfate Homologue Heparin**—Since the structural organization of the envelope glycoprotein E2 suggests an interaction with cellular GAGs (38), we first assessed whether E2 interacts with heparin. Heparin is not a constituent of cell membranes but is a close structural homologue of highly sulfated heparan sulfate, which is expressed in various forms on the surface of defined cells and extracellular matrices including hepatocytes (28). Using heparin complexed with BSA as a capture antigen in an ELISA, E2 showed a strong and concentration-dependent interaction with heparin. Heparin binding profiles of E2 from HCV-LPs and recombinant E2 had similar features (Fig. 1). By contrast, no E2 binding was observed to BSA-coated control ELISA plates, indicating that the observed interaction was specific in the established assay (Fig. 1). E2-heparin binding was subtype-independent since HCV-LP E2 from genotype 1a and 1b demonstrated a similar interaction with heparin (data not shown). With our heparin-capture ELISA under the conditions described above, no interaction between heparin and recombinant HCV non-structural proteins NS5A and NS5B could be detected (data not shown). These data indicate that E2 interacts specifically with the heparan sulfate homologue heparin *in vitro*.

To characterize the affinity of heparin-E2 interaction in detail, surface plasmon resonance (SPR) analysis was performed.

SPR allows a direct quantitative analysis of label-free molecular interactions in real-time. Highly purified BSA-heparin was covalently immobilized on a biosensor chip (42) and tested for binding of recombinant E2. A control flow cell (Fc1) was prepared similarly using BSA. As shown in the sensorgrams (Fig. 2), E2 bound dose-dependent to the heparin biosensor surface. E2-heparin association was demonstrated by the biosensor chip response following the initiation of sample injection. The maximal response reached 31 RU for 50 nM E2 and 365 RU for 100 nM E2 (Fig. 2). 180 s after sample injection, the sensor surface was regenerated using several wash buffers with high ionic strength. The biosensor chip response decreased to 21 RU and to 189 RU for 50 nM and 100 nM E2, respectively, on washing with 10  $\mu$ l of 2 M NaCl. Assuming a one-to-one interaction (Langmuir model) between the immobilized ligand (heparin) and soluble analyte (E2 protein), the calculation of the kinetic parameters for E2-heparin binding revealed a dissociation constant ( $K_D$ ) of  $5.2 \times 10^{-9}$  M ( $k_{on}$  of  $6.3 \times 10^{-4}$  M<sup>-1</sup> s<sup>-1</sup>,  $k_{off}$  of  $3.3 \times 10^{-4}$  s<sup>-1</sup>). These data demonstrate that E2 and heparin bind with a very high affinity.

**Heparin and Highly Sulfated Heparan Sulfate Inhibit Binding of Envelope Glycoprotein E2 to Human Cell Lines**—Since we observed a concentration-dependent interaction of HCV envelope glycoproteins with heparin we studied whether heparin and other soluble cell surface GAGs inhibit binding of HCV-LP to hepatoma and lymphoma cell lines. These cell lines have been shown to interact specifically with recombinant E2 protein, HCV-LPs, and virions and therefore represent a model for the study of the HCV-host cell membrane interaction (8–10, 18, 19, 46, 47). Furthermore, several studies have demonstrated evidence that the lymphoma cell lines MOLT-4 and Daudi are susceptible to low-level HCV infection (for review see Ref. 4). Evidence for HCV infection has also been demonstrated for HepG2 and HuH-7 cell lines, even though the levels of replication in these cells are too low to serve as a robust model for HCV infection (4). HepG2 cells have also been used to study HCV binding and entry (48). Preincubation of HCV-LPs with increasing concentrations of heparan sulfate-homologue heparin, resulted in a dose-dependent inhibition of HCV-LP E2 binding to HepG2 hepatoma and MOLT-4 lymphoma cells. At the highest heparin concentration (10  $\mu$ g/ml or 1  $\mu$ M) used in this study, HCV-LP binding to both HepG2 and MOLT-4 cells was inhibited more than 95% (Fig. 3). The heparin concentration required for a 50% inhibition of cellular binding ( $ID_{50}$ ) was in the low nanomolar range (0.003  $\mu$ g/ml or 0.3 nM for HCV-LP binding to HepG2 cells and 0.004  $\mu$ g/ml or 0.4 nM for HCV-LP binding to MOLT-4 cells, respectively, mean of three independent experiments). In contrast, preincubation of HCV-LPs with GAGs keratan sulfate, dermatan sulfate, chondroitin sulfate (Fig. 3) and dextran sulfate (data not shown) did not result in inhibition of HCV-LP binding. Interestingly, dermatan sulfate at a concentration of 10  $\mu$ g/ml enhanced HCV-LP E2 binding to MOLT-4 cells (Fig. 3). Specific inhibition of HCV-LP binding by heparin was also observed for the hepatoma cell line HuH-7 and Daudi B-lymphoma cells (data not shown). The inhibition of cellular binding of HCV-LPs of genotype 1a and 1b by heparin was similar, indicating that inhibition is genotype-independent (Fig. 3).

Since heparin is a structural homologue of highly sulfated heparan sulfate, we next assessed whether highly sulfated heparan sulfate purified from liver membranes was able to inhibit HCV-LP or recombinant E2 binding. To study the possible role of heparan sulfate sulfation in inhibition of viral envelope binding, a side-by-side analysis was performed using kidney-derived heparan sulfate. Liver- and kidney-derived heparan sulfates represent prototypes for "highly" and "nor-

<sup>2</sup> T. H. van Kuppevelt, unpublished results.

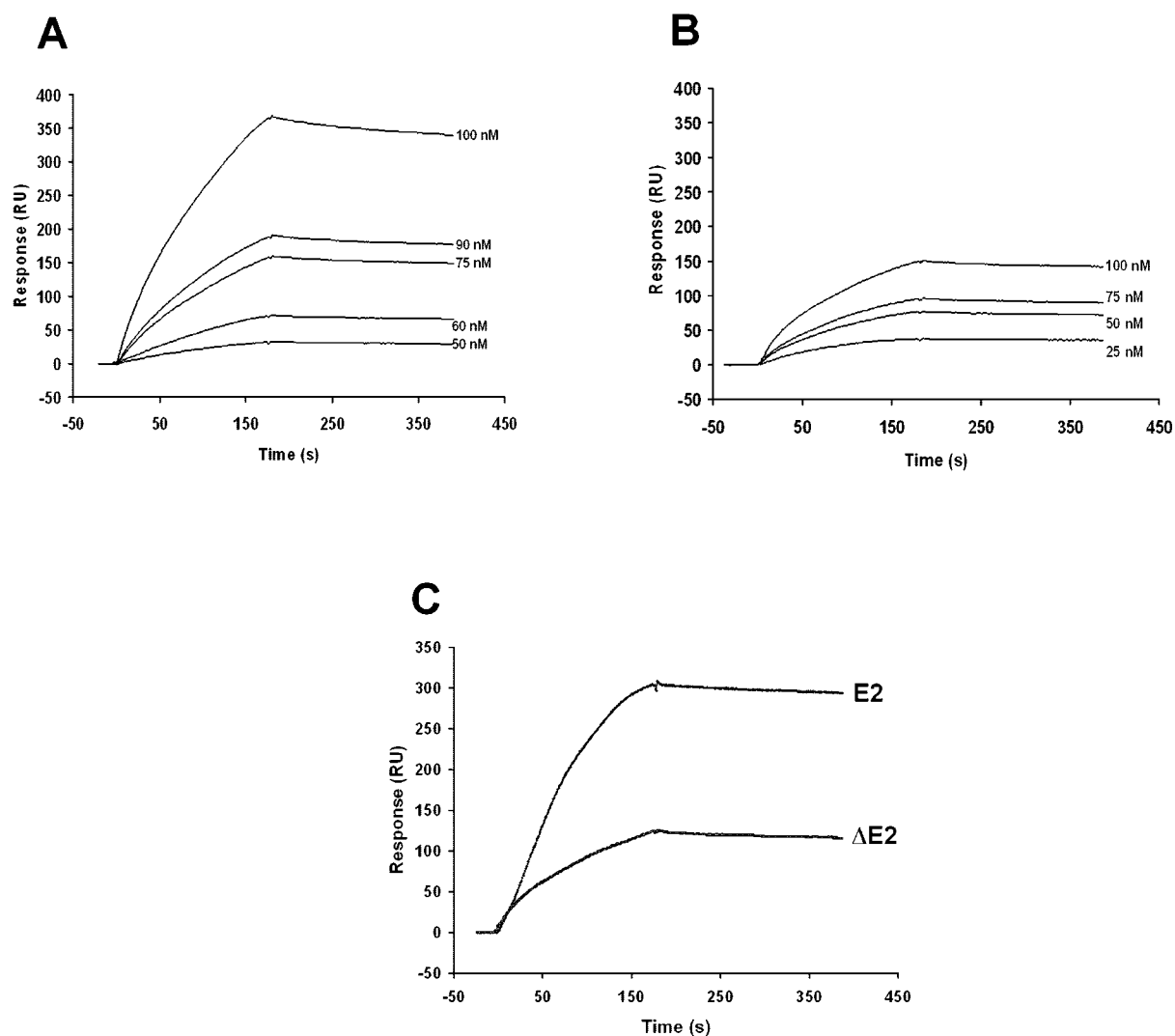


FIG. 2. **SPR analysis of E2-heparin interaction.** BSA-heparin or BSA was covalently immobilized onto the surface of biosensor chips as described under "Experimental Procedures." Subsequently, different concentrations of recombinant E2 were injected on the biosensor surface for 180 s at a flow rate of 10  $\mu$ l/min. The sensor surface was then regenerated by injecting with 10  $\mu$ l of 2 M NaCl as described under "Experimental Procedures." The biosensor chip response is indicated on the y-axis (measured in RU) as a function of time (x-axis) at 25  $^{\circ}$ C. The sensorgram shows the difference of BSA-heparin-coated chip response compared with BSA-coated control chip response following E2 injection. SPR analysis of E2 and  $\Delta$ E2 containing a deletion of hypervariable region 1 are shown in A and B. A side-by-side analysis of E2 and  $\Delta$ E2, both at 100 nM, is shown in panel C.

mally" sulfated heparan sulfates and have been successfully applied to characterize the role of sulfation for the interaction of heparan sulfate with other cellular ligands such as dengue virus (29, 40). The previously characterized structure has pointed to marked differences in disaccharide sulfation of these two molecules (40): Whereas liver heparan sulfate is characterized by a sulfate to disaccharide ratio of 1.05, kidney-derived heparan sulfate displays a sulfate to disaccharide ratio of only 0.60 (40). This marked difference is also reflected in the relative percentage of *N*- and *O*-sulfated disaccharides in the two molecules: the percentage of *N*-sulfated and *O*-sulfated disaccharides amounts to 42.0 and 62.6% for liver-heparan sulfate in contrast to 28.6 and 32.5% for kidney heparan sulfate (40). Furthermore, the comparative analysis of disaccharide composition revealed a major difference in the amount of trisulfated disaccharide  $\Delta$ UA2S-GlcNS6S. Whereas liver heparan sulfate contains a substantial amount of trisulfated disaccharide  $\Delta$ UA2S-GlcNS6S (21.2% of unsaturated disaccharides),  $\Delta$ UA2S-GlcNS6S is hardly detectable in kidney heparan sulfate (1.3% of unsaturated disaccharides; (40)).

As shown in Fig. 4, liver-derived, highly sulfated heparan sulfate strongly inhibited HCV-LP E2 binding to HepG2 cells

in a dose-dependent manner. By contrast, kidney-derived normally sulfated heparan sulfate did not inhibit HCV-LP binding. Similar findings were observed when recombinant E2 was used as a ligand for cellular binding. Heparin and highly sulfated liver-derived heparan sulfate strongly inhibited cellular binding of recombinant E2, while co-incubation of recombinant E2 with keratan sulfate, dermatan sulfate, chondroitin sulfate, and kidney-derived normally sulfated heparan sulfate did not affect recombinant E2 binding (Fig. 5B). Taken together, these data indicate that the level of heparan sulfate disaccharide sulfation plays an important role in mediating heparan sulfate-E2 interaction.

**Heparin-mediated Inhibition of Virus-like Particle Entry into Target Cells**—The next step after particle binding is uptake or entry of particles into the cell. Since virus envelope binding represents only the first step for the initiation of viral infection, it is of interest to study whether the interaction of HCV E2 with heparan sulfate is important for events downstream from envelope binding. A recent report has demonstrated envelope-dependent internalization of HCV-LPs into target cells (19). Therefore, we studied whether the heparan sulfate homologue heparin inhibits internalization of HCV-LPs into target cells.

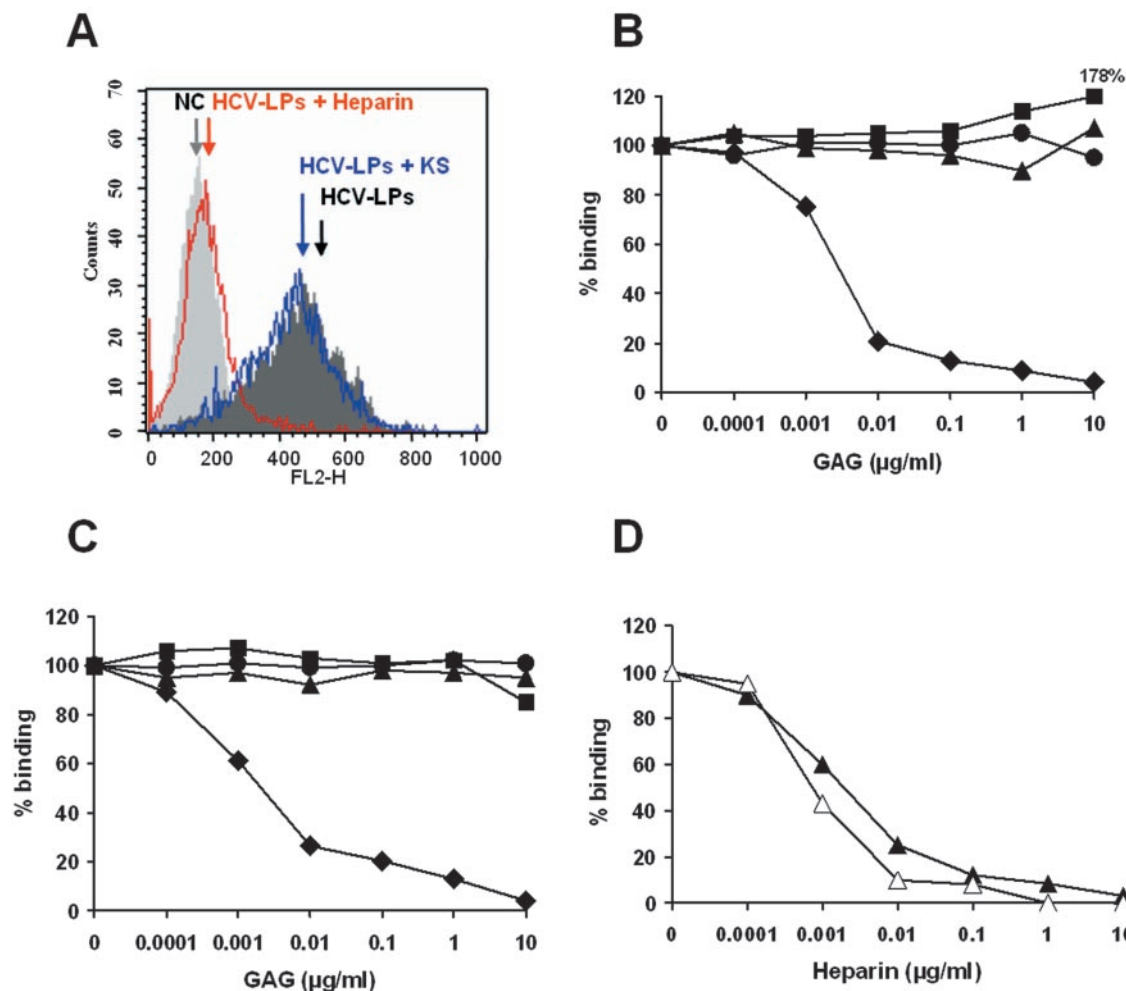


**FIG. 3. Cellular binding of HCV-LPs in the presence of soluble GAGs.** HCV-LPs were incubated with increasing concentrations of GAGs for 20 min at room temperature. HCV-LP/GAG complexes were added to the cells for 1 h at 4 °C. After extensive washing with PBS, cellular binding of HCV-LPs was quantified by flow cytometry using monoclonal anti-E2 and PE-conjugated anti-mouse IgG antibodies. **A**, flow cytometry histogram of HCV-LPs binding to MOLT-4 cells in the absence of GAGs (dark gray-shaded graphs), presence of heparin (final concentration 10 μg/ml; red lined, unshaded graph) or keratan sulfate (10 μg/ml, blue lined, unshaded graph). Background fluorescence (negative control, NC) was measured as described above using cells incubated with an insect cell control preparation. Fluorescence intensity (FL2-H) and relative cell number (counts) are shown on the x- and y-axis, respectively. **B** and **C**, binding of HCV-LPs to MOLT-4 (**B**) and HepG2 cells (**C**) in the presence of increasing concentrations of heparin (diamonds), keratan sulfate (triangles), dermatan sulfate (squares), or chondroitin sulfate (circles). Data are shown as percent binding relative to binding of HCV-LPs without GAGs (100%). **D**, cellular binding of HCV-LPs of different genotypes in the presence of heparin. HCV-LPs derived from cDNAs of HCV genotypes 1a (▲) and 1b (△) were preincubated with increasing concentrations of heparin. After addition of HCV-LP/heparin complexes to HepG2 cells, cellular HCV-LP binding was detected by flow cytometry as described above. Data show the mean of a representative experiment performed in duplicate.

Temperature-dependent HCV-LP entry into HepG2 cells was analyzed using anti-E2 specific immunofluorescence and confocal laser scanning microscopy. As shown in Fig. 6, incubation of HepG2 cells with HCV-LPs at 4 °C resulted in the exclusive detection of HCV-LP E2 on the cell surface, consistent with HCV-LP binding to the cell membrane. By contrast, incubation at 37 °C resulted in the translocation of E2 immunoreactivity into the cell consistent with HCV-LP entry. Following a preincubation of HCV-LPs with heparin and addition of heparin-HCV-LP complexes to HepG2 cells at 37 °C, HCV-LP E2 protein was neither detected as a ring-like structure at the cell surface nor as intracellular spots localized in the cytoplasm. These data indicate that heparin-mediated inhibition of binding may be sufficient to prevent HCV-LP envelope internalization.

**Highly Sulfated Cell Surface Heparan Sulfate Is a Binding Receptor for Envelope Glycoprotein E2**—To demonstrate that the inhibitory effect of heparin and highly sulfated heparan sulfate on envelope protein binding was due to competition with a similar molecular species on the target cell, hepatoma,

and lymphoma cell lines were treated with specific GAG lyases, followed by assessment of HCV-LP E2 binding. Pretreatment of MOLT-4 cells with heparinase I (degrading heparin and highly sulfated domains in heparan sulfate) almost completely abolished HCV-LP E2 binding (Fig. 7A). For HepG2 cells, an inhibition of HCV-LP E2 binding of 45–75% was observed. Pretreatment of cells with heparinase III (degrading heparan sulfate) markedly decreased HCV-LP E2 binding to MOLT-4 (maximum inhibition: 75%) and HepG2 cells (maximum inhibition: 42%). By contrast, degradation of other non-heparan sulfate GAGs by chondroitin lyase ABC (degrading chondroitin and dermatan sulfate) had little or no effect on HCV-LP E2 binding (Fig. 7A). Similar results were obtained when recombinant E2 was used as a ligand for cellular binding. Pretreatment of MOLT-4 cells with heparinases I and III (1 unit/ml) resulted in 68 and 42% inhibition of E2 binding, respectively (data not shown). These data are consistent with the hypothesis that sulfated motifs in heparan sulfate act as cellular receptor mediating binding of HCV E2 protein to target cells.

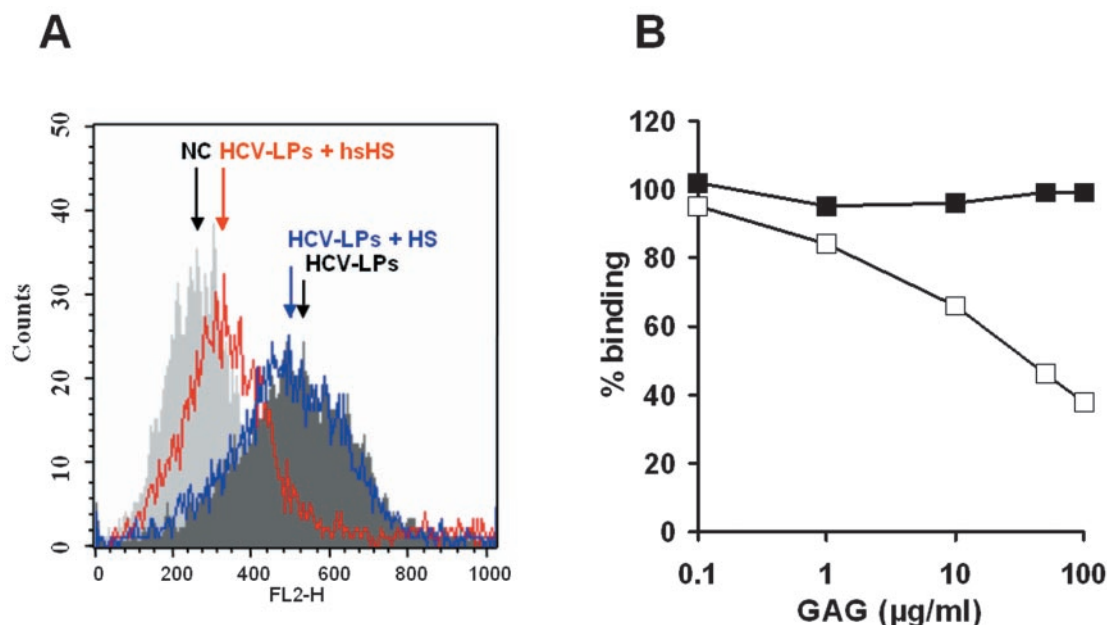


FIG. 4. **Binding of HCV-LPs to HepG2 cells in the presence of highly sulfated liver-derived and kidney-derived normally sulfated heparan sulfate.** *A*, flow histogram of HCV-LPs binding to HepG2 cells in the absence (dark gray shaded graph) or presence of highly sulfated heparan sulfate (final concentration, 100  $\mu\text{g/ml}$ ; red lined, unshaded graph) or normally sulfated heparan sulfate (final concentration 100  $\mu\text{g/ml}$ ; blue lined, unshaded graph). Background binding (negative control, NC) was measured as described in Fig. 3. *B*, comparative analysis of HCV-LP binding in the presence of increasing concentrations of normally sulfated kidney-derived (■) and highly sulfated liver-derived heparan sulfate (□). Data are shown as percent binding relative to binding of HCV-LPs without heparan sulfate (100%).

The experiments comparing highly sulfated and low-sulfate forms of heparan sulfate as inhibitors for E2 binding indicated that the degree of sulfation plays an important role in the E2-heparan sulfate interaction. To confirm that GAG sulfation is indeed required for HCV-LP E2 binding, we cultured HepG2 cells in the presence of sodium chlorate, an inhibitor of cellular sulfation. Exposure of HepG2 cells to sodium chlorate for 48 h was sufficient to inhibit HCV-LP E2 binding up to 80% (Fig. 7B). The specificity of this effect was confirmed by supplementing the sodium chlorate-treated cells with an excess of sodium sulfate that resulted in reconstitution of HCV-LP E2 binding (Fig. 7B). Cell viability was not affected by these agents based on unchanged flow cytometry light scatter (data not shown).

To investigate whether highly sulfated heparan sulfate is expressed on the cell surface of our target cells, we performed immunofluorescence of our target cell lines using a previously characterized single chain anti-heparan sulfate antibody (43). Immunostaining of cell surface heparan sulfate using phage display-derived monoclonal single-chain antibodies has been shown to represent a powerful tool for the structural characterization of tissue heparan sulfate topology and diversity (49). Antibody HS4C3 interacts with highly sulfated heparan sulfate and heparin but not with moderately sulfated heparan sulfate from tissues such as aorta (43). Furthermore, it does not react with *N*-sulfated, but *O*-desulfated heparan sulfate, nor with completely desulfated heparan sulfate or *N*-desulfated, but *O*-sulfated heparan sulfate confirming its specificity for heparan sulfate containing highly sulfated disaccharides (43). HS4C3 stained cell surface heparan sulfate on both HepG2 and MOLT-4 cells as shown by flow cytometry and immunofluorescence (Fig. 8; immunofluorescence for MOLT-4 cells not shown). These data indicate that highly sulfated heparan sulfate is exposed at the target cell surface.

To proof that our target cell lines indeed contain heparan sulfate with highly sulfated disaccharides, we analyzed the disaccharide composition of cell surface heparan sulfate by high performance liquid chromatography with post-column flu-

orescence detection (Fig. 9, Table I). Our detailed analysis confirmed the presence of highly sulfated disaccharides on the target cell membrane: The ratio of sulfates/disaccharides was 0.86 for MOLT-4 cells and 0.79 for HepG2 cells (Table I). The percentage of *N*-sulfated disaccharides was similar to liver-derived, highly sulfated heparan sulfate (40.5 and 40.2% *N*-sulfated/total disaccharides for HepG2 and MOLT-4 cells, respectively). Interestingly, the comparative disaccharide analysis demonstrated a markedly conserved disaccharide composition in the two target cell lines (Table I). Trisulfated disaccharide  $\Delta\text{UA}2\text{S-GlcNS}6\text{S}$ , an important constituent of liver-derived heparan sulfate and heparin, was detected in target cell heparan sulfate (9.9 and 6.7% of total unsaturated disaccharides for MOLT-4 and HepG2 cells respectively, Table I). These data clearly demonstrate that heparan sulfate of target cell lines MOLT-4 and HepG2 cells indeed contain highly sulfated disaccharides and therefore can be classified as highly sulfated heparan sulfate. The presence of highly sulfated disaccharides on the cell surface of target cells corroborates the hypothesis that highly sulfated heparan sulfate disaccharides on the target cell membrane act as cellular E2 binding molecules.

*E2 Hypervariable Region 1 (HVR-1) Is Important for E2-GAG Interaction*—To assess whether the E2 HVR-1 plays a role in mediating E2-heparan sulfate interaction, recombinant E2 containing a deletion of HVR-1 ( $\Delta\text{E}2$ ) was used as a ligand for heparin and cell surface interaction. A side-by-side-analysis of envelope protein-heparin interaction by SPR demonstrated a markedly decreased heparin binding of  $\Delta\text{E}2$  in comparison with E2 containing HVR-1 (Fig. 2).

To study whether the decrease in E2-heparin interaction is also reflected in cellular binding of E2 to target cells, we compared cellular binding of  $\Delta\text{E}2$  with E2 containing HVR-1. Similar to the results seen in SPR analysis,  $\Delta\text{E}2$  exhibited a markedly decreased ability to bind to MOLT-4 (Fig. 5A) and HepG2 cells (data not shown). These results suggest that E2 HVR-1 plays an important role in mediating E2-heparin and E2-cell surface heparan sulfate interaction.



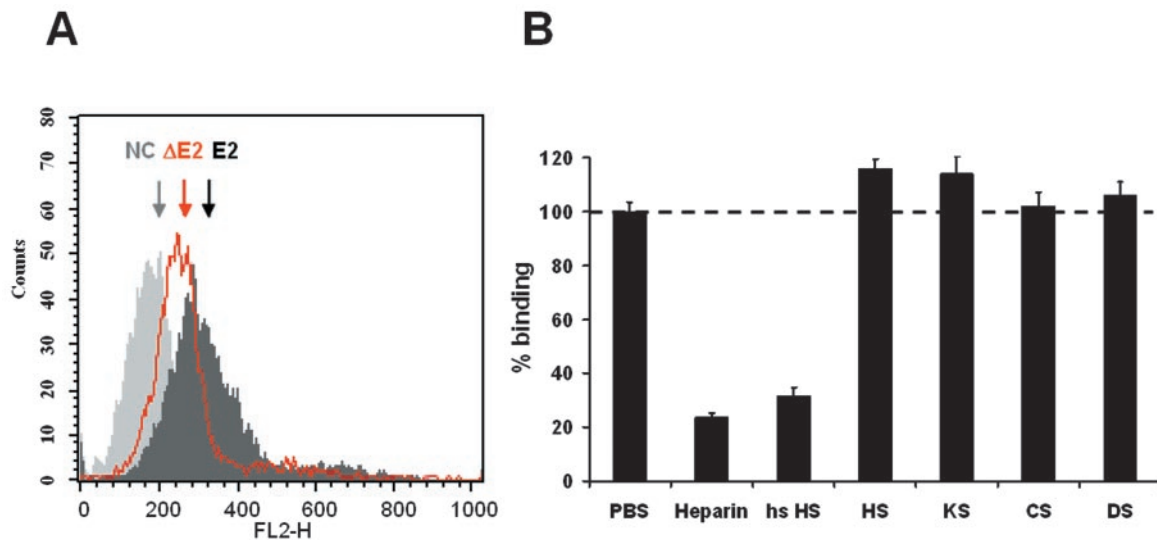


FIG. 5. *A*, flow cytometry histograms of E2 and  $\Delta$  E2 (containing a deletion of HVR-1) binding to MOLT-4 cells. MOLT-4 cells were incubated with recombinant envelope proteins as described under “Experimental Procedures” and binding was analyzed by flow cytometry as described in Fig. 3 (*NC*, negative control corresponding to cells incubated without envelope protein). *B*, cellular binding of recombinant E2 in the presence of soluble GAGs. Recombinant E2 was preincubated with heparin, normally sulfated heparan sulfate (*HS*), highly sulfated heparan sulfate (*hsHS*), keratan sulfate (*KS*), chondroitin sulfate (*CS*), or dermatan sulfate (*DS*) (10  $\mu$ g/ml). E2/GAG complexes were added to MOLT-4 cells and cellular E2 binding was quantified by flow cytometry as described in Fig. 3. Data are shown as percent binding (mean  $\pm$  S.D. of a representative experiment performed in triplicate) relative to binding of E2 without GAGs (100%).

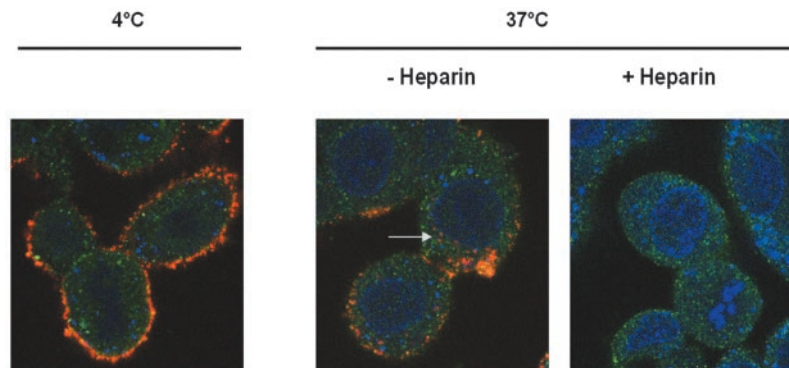


FIG. 6. **Heparin-mediated inhibition of virus-like particle entry into target cells.** HCV-LPs were preincubated with or without heparin as described under “Experimental Procedures.” HCV-LP binding was measured by incubation of HepG2 cells (grown on cover slides) with HCV-LP or HCV-LP-heparin complexes at 4  $^{\circ}$ C for 40 min (*left panel*). For temperature-dependent HCV-LP entry, cells were incubated for additional 60 min at 37  $^{\circ}$ C (*middle and right panels*). After removal of non-bound HCV-LPs by washing with ice-cold PBS, cells were fixed, permeabilized and stained for HCV-LP binding and entry using anti-E2 and Cy3-conjugated anti-mouse IgG antibodies. For the co-staining of the cytoskeleton, cells were co-incubated with a rabbit anti-actin and FITC-conjugated anti-rabbit IgG antibody. For staining of the nucleus, cells were incubated with DRAQ-5, a highly permeable DNA-interactive agent. Stained cells were analyzed using a laser scanning confocal microscope.

#### DISCUSSION

In this study, we demonstrate that the HCV envelope glycoprotein E2 interacts with defined cell surface heparan sulfate proteoglycans (HSPGs) and that this interaction mediates E2 binding to target cells. This conclusion is supported by four key experimental observations: (i) E2 demonstrated direct interaction with heparin, a structural homologue of highly sulfated heparan sulfate; (ii) binding of E2 could be specifically inhibited by highly sulfated heparan sulfate and heparin but not by other closely related soluble GAGs; (iii) partial enzymatic degradation of cellular heparan sulfate but not other closely related GAGs resulted in a marked reduction of E2 binding; (iv) level of heparan sulfate sulfation appeared to play a crucial role for E2 binding.

The mechanism of GAG-protein binding ranges from simple charge effects to highly specific receptor-like interactions as described for binding of several viral proteins to heparan sulfate (29, 31, 34, 35). The specific inhibition of E2 binding by defined GAGs, such as highly sulfated heparan sulfate and pre-treatment of cells by defined GAG lyases, provides evidence

that E2-heparan sulfate binding is not mediated exclusively by simple charge interactions, but most likely includes a specific interaction with a defined structure present in heparan sulfate. Our data indicate that disaccharide sulfation and composition of disaccharides are important factors for efficient GAG-E2 interaction. This hypothesis is supported by the following observations: (i) Only highly sulfated heparan sulfate and heparin inhibited E2 binding to target cells (Fig. 3–5); (ii) treatment of cells with heparinases and sulfation inhibitor strongly inhibited E2 binding (Fig. 7); (iii) target cells contained heparan sulfate with highly sulfated disaccharides representing possible binding sites for E2 (Figs. 8 and 9; Table I).

Heparin was much more potent in inhibiting E2 binding to target cells than heparan sulfate. This observation is best explained by the different structure of heparan sulfate and heparin. Heparin is characterized by a very high sulfation of disaccharides (between 2.12 and 2.66 sulfates/disaccharides, Refs. 50 and 51, compared with 1.05 sulfates/disaccharides for liver-derived heparan sulfate and 0.60 sulfates/disaccharides for kidney-derived heparan sulfate, Ref. 40). This difference is

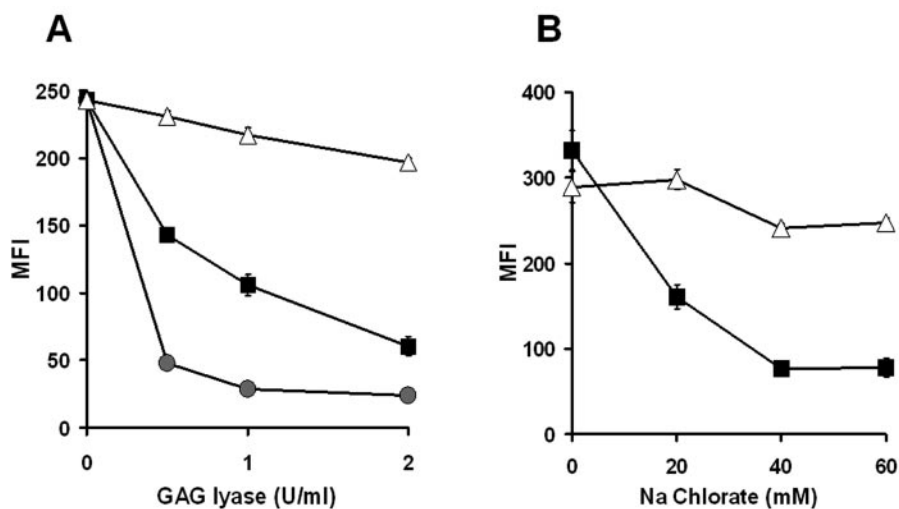


FIG. 7. *A*, role of cell surface heparan sulfate in HCV-LP E2 binding. MOLT-4 cells were preincubated with heparinase I (●), heparinase III (■), or chondroitin-ABC lyase (Δ) at concentrations indicated on the *x*-axis. Subsequently, HCV-LPs were added to cells and HCV-LP E2 binding was assessed by flow cytometry as described in Fig. 3. Data are shown as  $\Delta$  MFI (mean  $\pm$  S.D.) of a representative experiment performed in triplicate. *B*, HCV-LP binding and level of cellular sulfation. HepG2 cells were cultured for 48 h in the presence of the sulfation inhibitor sodium chlorate (0–60 mM). Replicate cells were supplemented with sodium sulfate (2 mM) to assess the sulfation specificity of any inhibition observed. HCV-LP E2 binding was assessed at the completion of the incubation period by flow cytometry. HCV-LP E2 binding is shown as  $\Delta$  MFI (mean  $\pm$  S.D.) of a representative experiment performed in triplicate. HCV-LP binding to cells incubated in sodium chlorate and further supplemented with sodium sulfate (Δ).

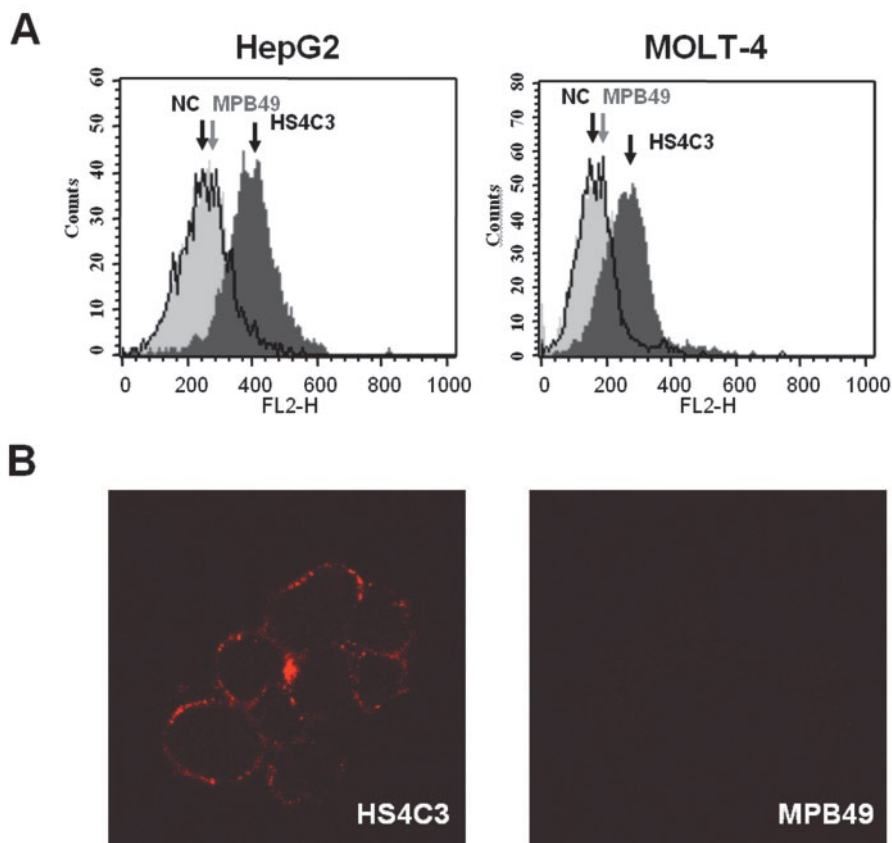


FIG. 8. **Immunostaining of highly sulfated cell surface heparan sulfate on target cell lines.** *A*, flow cytometry histograms of HepG2 (*left panel*) and MOLT-4 (*right panel*) cells stained with single chain anti-heparan sulfate antibody HS4C3 or single chain control antibody MPB49. Cells were incubated with primary and Cy3-labeled secondary antibodies as described under “Experimental Procedures” (NC, negative control corresponding to cells incubated with secondary antibody only). *B*, analysis of highly sulfated heparan sulfate expression on the cell surface of HepG2 cells by immunofluorescence. HepG2 cells were incubated with anti-heparan sulfate antibody HS4C3 (*left panel*) or control antibody MPB49 (*right panel*) and Cy3-labeled secondary antibody as described under “Experimental Procedures.” Stained cells were analyzed using laser scanning confocal microscopy.

also reflected by the percentage of N-sulfated disaccharides (88–98% for heparin, 42% for liver-derived heparan sulfate and 28.6% for kidney-derived heparan sulfate, Refs. 40 and 51). Furthermore, a comparative analysis of heparin and heparan sulfate composition revealed that the potency of GAG-induced inhibition of E2 binding did not only correlate with the total sulfate/disaccharide ratio but also with the presence of trisulfated disaccharide  $\Delta$ UA2S-GlcNS6S. Whereas heparin (derived

from bovine lung, used in this study) contains 86.2%  $\Delta$ UA2S-GlcNS6S (45), liver-derived heparan sulfate contains 21.2%  $\Delta$ UA2S-GlcNS6S (40). In contrast, kidney-derived heparan sulfate, not inhibiting cellular E2 binding, contains only 1.3%  $\Delta$ UA2S-GlcNS6S (40). Interestingly,  $\Delta$ UA2S-GlcNS6S was also detected on the cell surface of our target cell lines (Table I). These observations corroborate our hypothesis that total sulfation of disaccharides as well as the presence of defined dis-



accharides in heparin or heparan sulfate are important for GAG-E2 interaction. Further studies using chemically modified GAGs and defined disaccharides will allow mapping of the heparin and heparan sulfate-E2 binding motif(s).

To understand the mechanism of GAG-E2 interaction, it is also of interest to identify potential GAG binding sites on the viral envelope. The HCV N-terminal E2 region contains a stretch of highly conserved positively charged residues providing a potential binding site for heparan sulfate (38). Heparin-binding domains are located in protein regions rich in positively charged residues that can exhibit specific consensus structural motifs (52, 53). Deletion of the E2 HVR-1 resulted in a marked reduction of E2-heparin interaction as shown by SPR. These observations indicate that the E2 HVR-1 indeed plays a major role in envelope-GAG interaction as recently suggested (38). Since E2 containing a HVR-1 deletion still bound to heparin, it is conceivable that other envelope domains such as a recently suggested heparin binding motif at amino acids 559–614 close to the E2 C terminus (54), may also contribute to E2-heparin interaction.

For other viruses it has been shown that GAG-viral envelope glycoprotein is strain or isolate-dependent (55). By contrast, heparan sulfate-mediated envelope protein binding was observed for E2 proteins isolated from three different HCV isolates (HCV-J, H77C, European BE11 isolate) and genotypes

(1a, 1b) indicating that the heparan sulfate binding region is conserved among different HCV isolates and genotypes.

A key role for heparan sulfate in mediating E2 binding was demonstrated for both C-terminally truncated E2 monomers as well as for HCV-LP E2. The use of C-terminally truncated E2 protein as a surrogate ligand for HCV binding is limited by the fact that the proper conformation of the envelope protein requires the co-expression of both E1 and E2 proteins (56, 57). The signal sequences of E1 and E2 are important for membrane anchoring, heterodimerization, and membrane retention (58). In contrast to recombinant C-terminally truncated E2, HCV-LP E2 is present as an E1/E2 heterodimer expressed from a full-length E1/E2 cDNA. Several studies have demonstrated that HCV-LP contain E2 in a native conformation, which may resemble properly folded E2 in the virion (16, 18, 19). HCV-LPs and virions share distinct features in their cellular binding profiles, suggesting that cellular binding of HCV-LPs represents an appropriate model for the study of HCV-host cell membrane interaction (18, 19). The specific inhibition of HCV-LP binding by heparin and highly sulfated heparan sulfate, as well as the marked reduction of HCV-LP binding by pretreatment of cells with defined heparinases strongly suggests that highly sulfated heparan sulfate may act as a cellular molecule required for efficient binding of the HCV envelope to target cells.

Using anti-E2 specific immunofluorescence and confocal laser scanning microscopy we could demonstrate that heparin inhibits cellular binding and temperature-dependent internalization of HCV-LP E2. Using an envelope cell fusion assay, a recent study suggested that cell surface GAGs are involved in HCV cell fusion (59). Interestingly, heparan sulfate has been shown to interact specifically with the fusion domains of other viruses such as HIV glycoprotein gp41 (60). Taken together, these observations suggest that E2-cell surface heparan sulfate interaction may also play an important role in events downstream of cellular HCV envelope binding.

The direct study of the heparan sulfate-virion interaction is at present still limited by the lack of a cell culture system for the large scale synthesis of infectious virions and the difficulty of purifying HCV in large quantities from human sera or plasma. Recent advances in hepatocyte-based models for HCV infection (61–63) may help to clarify the role of cell surface heparan sulfate proteoglycans for the initiation of HCV infection in the future.

Heparan sulfate has been shown to serve as an important cellular binding molecule for several members of the *Flaviviridae* family such as Dengue (29–31), CSF (32), and TBE (33) viruses as well as herpes simplex virus 1 (34) human herpesvirus 8 (35) and papilloma virus (24). Interestingly, the affinity of HCV E2 protein for heparin ( $K_D$   $5.2 \times 10^{-9}$  M) was substantially stronger (10 fold) than that of other viral envelope glycoproteins, such as human herpes virus 8 envelope glycoprotein K8.1 ( $K_D$   $4.8 \times 10^{-8}$  M; Ref. 35, or Dengue virus envelope protein ( $K_D$   $5.6 \times 10^{-8}$  M; Ref. 64). This finding supports the specificity and potential biological relevance of the interactions observed.

It has been proposed that the affinity of viral surface molecules for heparan sulfate may determine viral tissue tropism and pathogenicity (36, 37). Recent investigations of the struc-

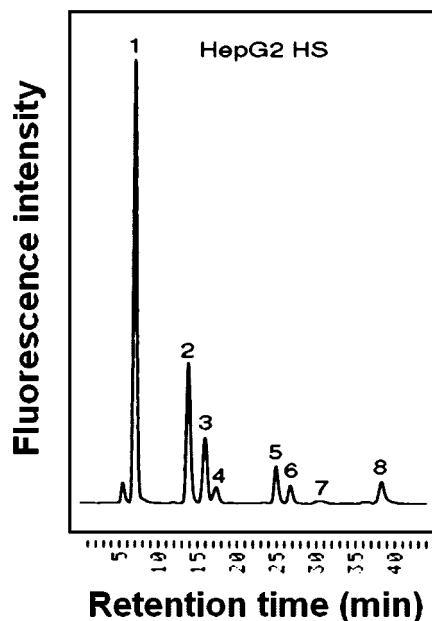


FIG. 9. Chromatogram of unsaturated disaccharides produced from heparan sulfate of HepG2 cells. Glycosaminoglycans were prepared from ~20 mg of lyophilized cells and analyzed by high performance liquid chromatography with post-column fluorescence detection. Unsaturated disaccharides produced enzymatically from 33% of heparan sulfate in the cells were loaded onto the HPLC column and separated as described under "Experimental Procedures." Peaks: 1,  $\Delta$ UA-GlcNAc; 2,  $\Delta$ UA-GlcNS; 3,  $\Delta$ UA-GlcNAc6S; 4,  $\Delta$ UA2S-GlcNAc; 5,  $\Delta$ UA-GlcNS6S; 6,  $\Delta$ UA2S-GlcNS; 7,  $\Delta$ UA2S-GlcNAc6S; 8,  $\Delta$ UA2S-GlcNS6S.

TABLE I

Compositions of unsaturated disaccharides produced from heparan sulfate of target cell lines HepG2 and MOLT-4

Heparan sulfate was isolated from freeze-dried cells and analyzed by high performance liquid chromatography with post-column fluorescence detection as described in "Experimental Procedures." The sulfates/disaccharide values were calculated from the disaccharide composition based on sulfation level of disaccharides.

Cell line	% Unsaturated disaccharide proportion								Sulfates / disaccharide
	$\Delta$ UA-GlcNAc	$\Delta$ UA-GlcNS	$\Delta$ UA-GlcNAc6S	$\Delta$ UA2S-GlcNAc	$\Delta$ UA-GlcNS6S	$\Delta$ UA2S-GlcNS	$\Delta$ UA2S-GlcNAc6S	$\Delta$ UA2S-GlcNS6S	
HepG2	46.1	22.9	9.9	2.9	6.5	4.4	0.6	6.7	0.79
MOLT-4	47.8	16.6	9.2	2.3	8.9	4.8	0.5	9.9	0.86

ture of heparan sulfate derived from a variety of sources have revealed high heterogeneity, expressed as differences in primary sequence and the pattern and level of sulfation (40, 49, 65). These tissue- and species-specific differences may contribute to target cell recognition and virus attachment (36, 66). Our own observation, demonstrating that the level of heparan sulfation plays an important role for mediating E2 binding, may have important implications for the understanding of HCV tropism. HCV-E2 binding has been demonstrated only for defined human cell lines and hepatocytes (8, 11, 18, 19). It is therefore conceivable that tissue- and species-specific heparan sulfate patterns including the level of sulfation, may play an important role for HCV binding and tropism.

The initial step in the viral life cycle is the attachment of the virion to the host cell membrane. Frequently several cellular molecules are involved in mediating virus binding and entry. Cell surface candidate molecules mediating HCV binding include CD81 on lymphocytes (10), or cell surface proteins involved in lipoprotein uptake such as LDL-receptor (12) or human scavenger receptor B1 (14) on hepatocytes. In conclusion, we propose that highly sulfated heparan sulfate may serve as the initial docking site for HCV attachment. The virus may then be transferred to a second high affinity receptor, triggering entry.

E2-heparan sulfate interaction may also represent a potential target for novel antiviral strategies. Interestingly, heparin inhibited HCV-LP binding in concentrations similar to concentrations used in humans for the treatment of coagulation disorders. Development of heparin-derived molecules inhibiting E2-heparan sulfate interaction specifically and potently may represent a novel concept of the treatment of HCV infection.

**Acknowledgments**—We thank M. Follo (Core Facility, Dept. of Medicine I, University of Freiburg, Freiburg, Germany) for performing confocal laser scanning microscopy. P. Schürmann and B. Gißler are gratefully acknowledged for excellent technical assistance.

#### REFERENCES

- Choo, Q.-L., Kuo, A., Weiner, A. J., Overby, L. R., Bradley, D. W., and Houghton, M. (1989) *Science* **244**, 359–362
- Lauer, G. M., and Walker, B. D. (2001) *N. Engl. J. Med.* **345**, 41–52
- Di Bisceglie, A. M., and Hoofnagle, J. H. (2002) *Hepatology* **36**, S121–127
- Bartenschlager, R., and Lohmann, V. (2000) *J. Gen. Virol.* **81**, 1631–1648
- Major, M. E., Rehmann, B., and Feinstone, S. M. (2001) in *Fields Virology* (Knipe, D. M., Howley, P. M., Griffin, D. E., Lamb, R. A., Martin, M. A., Roizman, B., and Straus, S. E., eds) Vol. 1, 4th Ed., pp. 1127–1161, Lippincott Williams & Wilkins, Baltimore
- Lindenbach, B. D., and Rice, C. M. (2001) in *Fields Virology* (Knipe, D. M., Howley, P. M., Griffin, D. E., Lamb, R. A., Martin, M. A., Roizman, B., and Straus, S. E., eds) Vol. 1, 4th Ed., pp. 991–1041, Lippincott Williams & Wilkins, Baltimore
- Shimizu, Y. K., Feinstone, S. M., Kohara, M., Purcell, R., and Yoshikura, H. (1996) *Hepatology* **23**, 205–209
- Rosa, D., Campagnoli, S., Moretto, C., Guenzi, E., Cousens, L., Chin, M., Dong, C., Weiner, A., Lau, J. Y. N., Choo, Q.-L., Chien, D., Pileri, P., Houghton, M., and Abrignani, S. (1996) *Proc. Natl. Acad. Sci. U. S. A.* **93**, 1759–1763
- Flint, M., and McKeating, J. A. (2000) *Rev. Med. Virol.* **10**, 101–117
- Pileri, P., Uematsu, Y., Campagnoli, S., Galli, G., Falugi, F., Petracca, R., Weiner, A. J., Houghton, M., Rosa, D., Grandi, G., and Abrignani, S. (1998) *Science* **282**, 938–941
- Flint, M., Maidens, C. M., Loomis-Price, L. D., Shotton, C., Dubuisson, J., Monk, P., Hittingbottom, A., Levy, S., and McKeating, J. (1999) *J. Virol.* **73**, 6235–6244
- Agnello, V., Abel, G., Elfahal, M., Knight, G. B., and Zhang, Q. X. (1999) *Proc. Natl. Acad. Sci. U. S. A.* **96**, 12766–12771
- Saunier, B., Triyatni, M., Ulianich, L., Maruvada, P., Yen, P., and Kohn, L. D. (2003) *J. Virol.* **77**, 546–559
- Scarselli, E., Ansuini, H., Cerino, R., Roccasecca, R. M., Acali, S., Filocamo, G., Traboni, C., Nicosia, A., Cortese, R., and Vitelli, A. (2002) *EMBO J.* **21**, 5017–5025
- Baumert, T. F., Ito, S., Wong, D., and Liang, T. J. (1998) *J. Virol.* **72**, 3827–3836
- Clayton, R. F., Owsianka, A., Aitken, J., Graham, S., Bhella, D., and Patel, A. H. (2002) *J. Virol.* **76**, 7672–7682
- Owsianka, A., Clayton, R. F., Loomis-Price, L. D., McKeating, J. A., and Patel, A. H. (2001) *J. Gen. Virol.* **82**, 1877–1883
- Wellnitz, S., Klumpp, B., Barth, H., Ito, S., Depla, E., Dubuisson, J., Blum, H. E., and Baumert, T. F. (2002) *J. Virol.* **76**, 1181–1193
- Triyatni, M., Saunier, B., Maruvada, P., Davis, A. R., Ulianich, L., Heller, T., Patel, A., Kohn, L. D., and Liang, T. J. (2002) *J. Virol.* **76**, 9335–9344
- Triyatni, M., Vergalla, J., Davis, A. R., Hadlock, K. G., Fong, S. K., and Liang, T. J. (2002) *Virology* **298**, 124–132
- Blanchard, E., Brand, D., Trassard, S., Goudeau, A., and Roingard, P. (2002) *J. Virol.* **76**, 4073–4079
- Ezelle, H. J., Markovic, D., and Barber, G. N. (2002) *J. Virol.* **76**, 12325–12334
- Xiang, J., Wunschmann, S., George, S. L., Klinzman, D., Schmidt, W. N., LaBrecque, D. R., and Stapleton, J. T. (2002) *J. Med. Virol.* **68**, 537–543
- Groglou, T., Florin, L., Schafer, F., Streeck, R. E., and Sapp, M. (2001) *J. Virol.* **75**, 1565–1570
- Gilbert, J. M., and Greenberg, H. B. (1998) *J. Virol.* **72**, 5323–5327
- Combata, A. L., Touze, A., Bousarhin, L., Christensen, N. D., and Coursaget, P. (2002) *J. Virol.* **76**, 6480–6486
- Tamura, M., Natori, K., Kobayashi, M., Miyamura, T., and Takeda, N. (2000) *J. Virol.* **74**, 11589–11597
- Bernfield, M., Gotte, M., Park, P. W., Reizes, O., Fitzgerald, M. L., Lincoff, J., and Zako, M. (1999) *Annu. Rev. Biochem.* **68**, 729–777
- Chen, Y., Maguire, T., Hileman, R. E., Fromm, J. R., Esko, J. D., Linhardt, R. J., and Marks, R. M. (1997) *Nat. Med.* **3**, 866–871
- Hilgard, P., and Stockert, R. (2000) *Hepatology* **32**, 1069–1077
- Germi, R., Crance, J. M., Garin, D., Guimet, J., Lortat-Jacob, H., Ruigrok, R. W., Zarski, J. P., and Drouet, E. (2002) *Virology* **292**, 162–168
- Hulst, M. M., van Gennip, H. G., Vlot, A. C., Schooten, E., de Smit, A. J., and Moormann, R. J. (2001) *J. Virol.* **75**, 9585–9595
- Mandl, C. W., Kroschewski, H., Allison, S. L., Kofler, R., Holzmann, H., Meixner, T., and Heinz, F. X. (2001) *J. Virol.* **75**, 5627–5637
- Shukla, D., Liu, J., Blaiklock, P., Shworak, N. W., Bai, X., Esko, J. D., Cohen, G. H., Eisenberg, R. J., Rosenberg, R. D., and Spear, P. G. (1999) *Cell* **99**, 13–22
- Birkmann, A., Mahr, K., Ensser, A., Yaguboglu, S., Titgemeyer, F., Fleckenstein, B., and Neipel, F. (2001) *J. Virol.* **75**, 11583–11593
- Putnak, J. R., Kanasa-Thanan, N., and Innis, B. L. (1997) *Nat. Med.* **3**, 828–829
- Shukla, D., and Spear, P. G. (2001) *J. Clin. Invest.* **108**, 503–510
- Penin, F., Combet, C., Germanidis, G., Frainais, P. O., Deleage, G., and Pawlotsky, J. M. (2001) *J. Virol.* **75**, 5703–5710
- van Doorn, L. J., van Hoek, K., de Martinoff, G., Bosman, F., Stuyver, L., Kos, T., Frantzen, I., Sillekens, P., Maertens, G., and Quint, W. (1997) *J. Med. Virol.* **52**, 441–450
- Toida, T., Yoshida, H., Toyoda, H., Koshiishi, I., Imanari, T., Hileman, R. E., Fromm, J. R., and Linhardt, R. J. (1997) *Biochem. J.* **322**, 499–506
- Baumert, T. F., Wellnitz, S., Aono, S., Sato, J., Herion, D., Tilman Gerlach, J., Pape, G. R., Lau, J. Y., Hoofnagle, J. H., Blum, H. E., and Liang, T. J. (2000) *Hepatology* **32**, 610–617
- Zhang, F., Fath, M., Marks, R., and Linhardt, R. J. (2002) *Anal. Biochem.* **304**, 271–273
- van Kuppevelt, T. H., Dennissen, M. A., van Venrooij, W. J., Hoet, R. M., and Veerkamp, J. H. (1998) *J. Biol. Chem.* **273**, 12960–12966
- Toyoda, H., Nagashima, T., Hirata, R., Toida, T., and Imanari, T. (1997) *J. Chromatogr. B Biomed. Sci. Appl.* **704**, 19–24
- Toida, T., Huang, Y., Washio, Y., Maruyama, T., Toyoda, H., Imanari, T., and Linhardt, R. J. (1997) *Anal. Biochem.* **251**, 219–226
- Wunschmann, S., Medh, J. D., Klinzmann, D., Schmidt, W. N., and Stapleton, J. T. (2000) *J. Virol.* **74**, 10055–10062
- Hamaia, S., Li, C., and Allain, J. P. (2001) *Blood* **98**, 2293–2300
- Andre, P., Komurian-Pradel, F., Deforges, S., Perret, M., Berland, J. L., Sodoyer, M., Pol, S., Brechet, C., Paranhos-Baccala, G., and Lotteau, V. (2002) *J. Virol.* **76**, 6919–6928
- Dennissen, M. A., Jenniskens, G. J., Pieffers, M., Versteeg, E. M., Petitou, M., Veerkamp, J. H., and van Kuppevelt, T. H. (2002) *J. Biol. Chem.* **277**, 10982–10986
- Volpi, N. (1993) *Carbohydr. Res.* **247**, 263–278
- Volpi, N. (1999) *Anal. Biochem.* **273**, 229–239
- Cardin, A. D., and Weintraub, H. J. (1989) *Arteriosclerosis* **9**, 21–32
- Margalit, H., Fischer, N., and Ben-Sasson, S. A. (1993) *J. Biol. Chem.* **268**, 19228–19231
- Yagnik, A.-T., Lahm, A., Meola, A., Roccasecca, R. M., Ercole, B. B., Nicosia, A., and Tramontano, A. (2000) *Proteins* **40**, 355–366
- Zhang, Y. J., Hatzioannou, T., Zang, T., Braaten, D., Luban, J., Goff, S. P., and Bieniasz, P. D. (2002) *J. Virol.* **76**, 6332–6343
- Patel, J., Patel, A. H., and McLauchlan, J. (2001) *Virology* **279**, 58–67
- Op De Beeck, A., Montserret, R., Duvet, S., Cocquerel, L., Cacani, R., Barberot, B., Le Maire, M., Penin, F., and Dubuisson, J. (2000) *J. Biol. Chem.* **275**, 31428–31437
- Cocquerel, L., Op de Beeck, A., Lambot, M., Roussel, J., Delgrange, D., Pillez, A., Wychowski, C., Penin, F., and Dubuisson, J. (2002) *EMBO J.* **21**, 2893–2902
- Takikawa, S., Ishii, K., Aizaki, H., Suzuki, T., Asakura, H., Matsuura, Y., and Miyamura, T. (2000) *J. Virol.* **74**, 5066–5074
- Cladera, J., Martin, I., and O'Shea, P. (2001) *EMBO J.* **20**, 19–26
- Zhao, X., Tang, Z. Y., Klumpp, B., Wolff-Vorbeck, G., Barth, H., Levy, S., von Weizsacker, F., Blum, H. E., and Baumert, T. F. (2002) *J. Clin. Invest.* **109**, 221–232
- Castet, V., Fournier, C., Soulier, A., Brillet, R., Coste, J., Larrey, D., Dhumeaux, D., Maurel, P., and Pawlotsky, J. M. (2002) *J. Virol.* **76**, 8189–8199
- Mercer, D. F., Schiller, D. E., Elliott, J. F., Douglas, D. N., Hao, C., Rinfret, A., Addison, W. R., Fischer, K. P., Churchill, T. A., Lakey, J. R., Tyrrell, D. L., and Kneteman, N. M. (2001) *Nat. Med.* **7**, 927–933
- Marks, R. M., Lu, H., Sundaresan, R., Toida, T., Suzuki, A., Imanari, T., Hernaiz, M. J., and Linhardt, R. J. (2001) *J. Med. Chem.* **44**, 2178–2187
- Kim, C. W., Goldberger, O. A., Gallo, R. L., and Bernfield, M. (1994) *Mol. Biol. Cell* **5**, 797–805
- Bergstrom, T., Trybala, E., and Spillmann, D. (1997) *Nat. Med.* **3**, 1177